JOURNAL OF MATERIALS SCIENCE 4 (1969) 396–404

The Electrical Properties of Plastically Bent p-Type Indium Antimonide Between 50 and 200° K

U. BAITINGER*, J. ARNDT, D. SCHNEPF
Institut für Halbleitertechnik, Universität Stuttgart, Germany

Received 4 November 1968

A special technique of plastic bending at elevated temperatures was applied to introduce, into a pair of simultaneously deformed, weakly p-doped, InSb single crystal bars, an excess, of indium and antimony dislocations, respectively. Hall coefficient and electrical conductivity of specimens containing an excess of In or Sb dislocations, of annealed control specimens, and of the Ge-doped starting material were measured between 50 and 200° K. Indium dislocations in Ge-doped InSb show not only an acceptor, but also a donor action; Sb dislocations show only an acceptor action. The electrostatic charge of the dislocations due to dislocation-impurity interaction has more influence on the measured energy level of indium dislocation states than on those of antimony. These results may be explained by assuming an energy level scheme in which the energy level of the indium dislocation states lies above and that of the antimony dislocation states below the acceptor level of the Ge impurity atoms.

1. Introduction

The electrical properties of semiconductors are determined by lattice defects at temperatures below that of the intrinsic conduction. These materials are therefore particularly suitable for study of the electrical effects of dislocations, which may be introduced into a single crystal by plastic deformation. Since each crystal contains on principle a certain number of different types of lattice defects (such as point defects), the study of one special type of defect (such as linear defects in this paper) always includes its interactions with other types. This paper will especially deal with the interaction between dislocations and impurity atoms.

The study of dislocations in polar crystals, such as III-V compounds, is of special interest since it is possible to distinguish in these crystals different kinds of dislocation of opposite sign whose electrical effects are expected to be different. In the sphalerite structure for example, two 60° dislocations of opposite sign have extra half-planes ending with a row of α and β atoms, respectively [1].

When plastic deformation is carried out by bending, it is possible to introduce an excess of either α- or β-dislocations depending on the bending direction relative to the stacking sequence of the slip planes [2].

Indium antimonide (InSb), which crystallises in the sphalerite structure, was chosen in order to have available a maximum of results on the undeformed material, since most of the theoretical and experimental work carried out on III-V compounds deals with this substance.

The electrical effects of dislocations in InSb have already been studied by several authors [3-11], but the experimental results and their interpretations are quite different. Bell *et al* [11] summarised the results obtained by previous authors and re-examined the problem. Their Hall coefficient and electrical conductivity measurements were carried out at only two fixed points of temperature: at room temperature and at liquid-nitrogen temperature. But, as will be shown below, the variation with temperature of these values is really complicated and interactions between dislocations and impurity atoms

*Present address: IBM Laboratorien, D703 Böblingen, Schönaicher First, Dept. 785, Germany.

may only be understood when their dependence upon temperature is known.

Therefore, we measured the Hall coefficient and electrical conductivity of specimens containing an excess of In and Sb dislocations, respectively, of annealed control specimens, and of the starting material between 50 and 200° K. We applied a special technique of plastic bending at elevated temperatures, to introduce, into a pair of simultaneously deformed, weakly p-doped, InSb single crystal bars, an excess of In and Sb dislocations, respectively, by bending to equal but opposite curvature without any essential chemical contamination.

2. Experimental Procedure

2.1. Possible Deformation Methods

The following methods of plastic deformation were considered for this investigation:

(*a*) *Plastic deformation by uniaxial compression.* Relatively high dislocation densities are introduced which have to be evaluated after deformation by chemical etching techniques (summarised by Amélinckx [12]). Dislocations with edge and/or screw components are introduced. The identification of the predominant dislocation type is difficult since the slip processes are complex.

(*b*) *Plastic deformation by torsion.* Dislocations with large screw and small edge components are introduced. The dislocation densities are relatively low. The geometrical arrangement of the dislocations is complex. The identification of the dislocation types is difficult.

(*c*) *Plastic deformation by bending.* Medium dislocation densities are introduced which are inversely proportional to the radius of curvature according to the relation of Nye [13]. The dislocation density may be dosed by proper choice of the radius of curvature and verified after deformation by chemical etching techniques. The slip processes of this particular method of deformation are well arranged. By a proper crystallographic orientation of the specimen cut from the as-grown single crystal, the number of activated slip planes may be predetermined as well as the sign and atom configuration of the majority of dislocations by the choice of the bending direction relative to the stacking sequence of the slip planes [2]. The identification of the dislocation types and their geometrical arrangement is possible by chemical techniques. On average, the dislocations run parallel to the bend axis [7].

Method (*a*) is not applicable to InSb when the electrical effects of dislocations are to be investigated, since, according to Duga *et al* [14], during deformation by uniaxial compression ionised vacancies and interstitials are introduced in approximately equal densities whose electrical effects are predominant and obscure those of the dislocations.

Method (*b*) seems to offer the possibility of investigating the electrical effects of the lattice distortions around the dislocations, since screw dislocations possess no dangling bond electrons. However, it is impossible to introduce an excess of dislocations without any dangling bond electrons, i.e. without any edge component.

Therefore, method (*c*) was chosen to introduce dislocations into InSb single crystals.

2.2. Techniques Used

Single crystals grown by the Czochralski method were oriented by X-rays and specimens in the shape of bars $3.5 \times 3.5 \times 15$ mm^3 were cut in proper crystallographic directions (see section 3.1.2.) by means of a tungsten wire saw. The specimens were etched in modified CP4 [15] to remove the surface layer of high dislocation density. Since the acid etch CP4 attacks Sb atoms preferentially, the surface stoichiometry was restored by the subsequent alkaline etch H-100 [16]. This etch contains complexing agents to eliminate metallic ion adsorption. Before, between, and after the etching processes the specimens were rinsed in de-ionised water. They were then preserved in methanol until being put into the bending apparatus.

The principle of the bending apparatus is shown in fig. 1. A graphite bending jig is placed under a water-cooled helmet and is heated up by a graphite winding*. The jig is exchangeable according to the desired radius of curvature. The apparatus may be evacuated and filled with a gas previously purified by a cooling trap. The temperature is controlled by means of a thermistor bridge. Before each bending process, the graphite components were purified by annealing them three times under high vacuum at 1050° C to remove occluded gas (particularly O_2) and adsorbed impurities. Before the samples were set into the apparatus, N_2 gas was let in under normal pressure to prevent the repeated absorption of O_2 by the graphite.

A pair of adjacent bars cut from the as-grown crystal was set into the bending jig with

*The helmet and graphite winding are not shown in fig. 1.

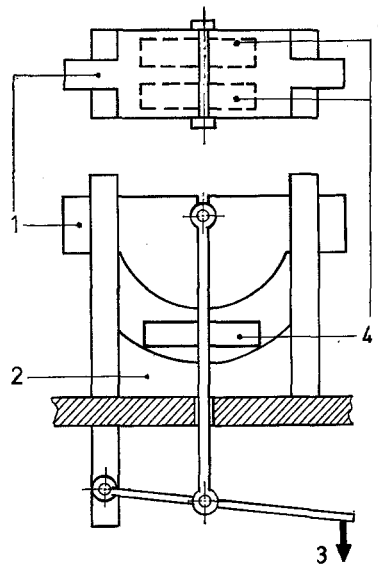

Figure 1 Schematic drawing of the bending apparatus. 1,2, graphite bending jig (exchangeable according to the desired radius of curvature), 3, constant load, 4, specimens.

opposite stacking sequence of the (111) slip planes. This had been identified after the etching of the samples in modified CP4 by the following method.

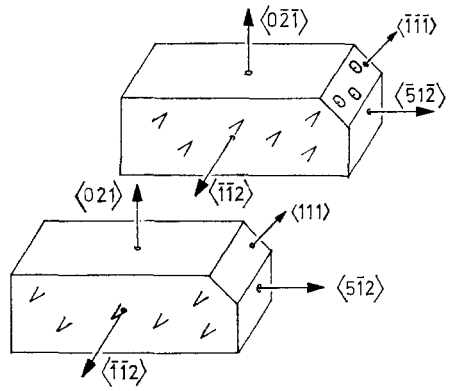

Figure 2 Identification of the crystallographic polarity by means of etch pits on (111) and (112) planes.

When the samples were sectioned along (111) planes as shown in fig. 2, circular etch pits are produced only on $\{\bar{1}\,\bar{1}\,\bar{1}\}$ faces, but not on $\{1\,1\,1\}$ faces [17]. The arrow-shaped etch pits produced on the (112) lateral faces are all pointing in the same direction, i.e. in the $<\bar{1}\,\bar{1}\,1>$ direction as shown in fig. 2. The latter etch pits are developed in sufficient quantities on the (112) faces of the unbent samples thus allowing the identification of their crystallographic polarity. A pair of samples was then arranged in the bending jig according to fig. 2.

InSb may be deformed plastically at temperatures

$$T > \frac{2}{3} T_f$$

[18]. With the melting point $T_f = 798°$ K of InSb we get

$$t > 260° \text{ C}.$$

At elevated temperatures, the diffusion velocities and solubilities of electrically active impurities, however, increase rapidly so that an undesired increase of the chemical donor and/or acceptor density may occur during plastic bending. In addition, impurity atoms diffuse preferentially along dislocations into the crystal volume, since dislocations are surrounded by regions of elastic strain.

Of the rapidly diffusing elements of high solubility in InSb, the acceptors Cd and Zn are to be particularly considered, since they are present even in undoped InSb single crystals of high purity [19]. Boltaks *et al* [20] found that the maximum solubility of Cd in InSb occurred at 400° C. Above and below this temperature, the solubility decreases rapidly. The maximum solubility of Zn in InSb lies, according to Gusev *et al* [21], at 445° C.

In addition, the different exodiffusion coefficients of In and Sb atoms have to be considered, when InSb is thermally treated under vacuum. According to Dzhanelidze *et al* [22], the ratio of the exodiffusing atoms $N_{Sb}:N_{In}$ attains a maximum of 3.7 at 460° C, i.e. an excess of electrically active Sb vacancies is introduced into the bulk and the surface is enriched with In atoms which may lead to an increased surface conductivity.

In order to minimise the chemical contamination during the bending process, the specimens were heated up to a final temperature $t_b = 300°$ C in an artificial atmosphere of 92% N_2 + 8% H_2 at a pressure of 1 torr. The final temperature was reached after approximately 10 min. The pressure was then reduced as low as possible (to about 10^{-6} torr) and the pair of samples was bent simultaneously under a constant load of 3 kg to equal but opposite curvature until the desired radius was attained, thus introducing an excess of In and Sb dislocations, respectively. A third adjacent bar cut from the as-grown crystal

was annealed together with the bent samples to control the chemical contamination during the thermal treatment. The time of cooling to room temperature was about 20 min.

From the bent samples, straight bars 2 × 2 × 10 mm³ were prepared by grinding, etched in modified CP4 to remove the damaged and contaminated surface layer, and re-etched in H100 to restore the surface stoichiometry in order to prevent an increased surface conductivity. For current feed, Indium metal contacts were soldered to the end surfaces of the bars. These contacts were purely ohmic within the analysed temperature range. The treatment of the unbent samples was analogous.

3. Results

3.1. Crystallographic Considerations

3.1.1. Identification of Majority Dislocations

The character of majority dislocations, predetermined by identification of the stacking sequence and proper choice of the bending direction, was verified after plastic deformation by selective etching.

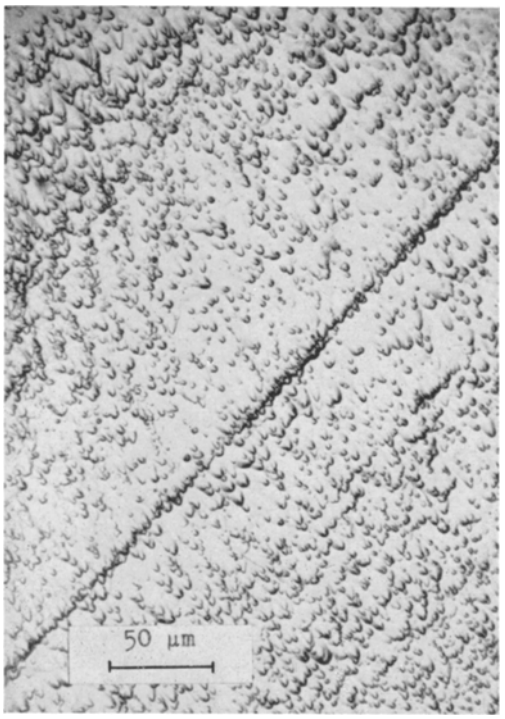

Figure 3 Single slip. The arrow-shaped etch pits revealed by modified CP4 on a (1 1 2) lateral face are perpendicular to the lines of intersection between the activated (1 1 1) slip plane system and the etched face of the sample. The etch pits are attributed [17] to In dislocations.

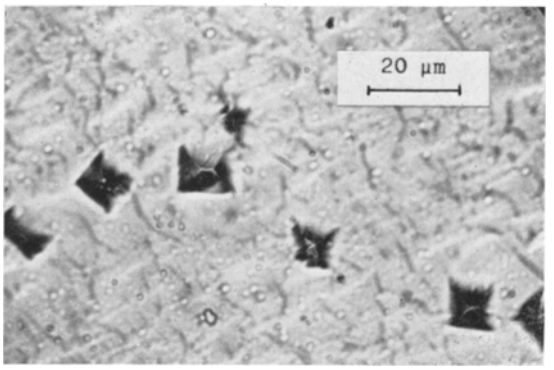

Figure 4 Etch pits on a (1 1 2) lateral face of the crystal bar attributed [23] to Sb dislocations.

The modified CP4 mentioned in section 2.2. attacks preferentially at In dislocations [17]. An etch containing n-butylthiobutane [23] produces etch pits attributed to Sb dislocations. Fig. 3 shows etch pits on a (1 1 2) face which is penetrated by In dislocations. Fig. 4 shows Sb dislocation etch pits on a (1 1 2) face, both revealed by the above mentioned etching techniques.

3.1.2. Slip Systems

Well-arranged slip processes and unambiguous types of majority dislocations are attained by single slip [18]. The crystallographic orientation of the samples is shown in fig. 5.

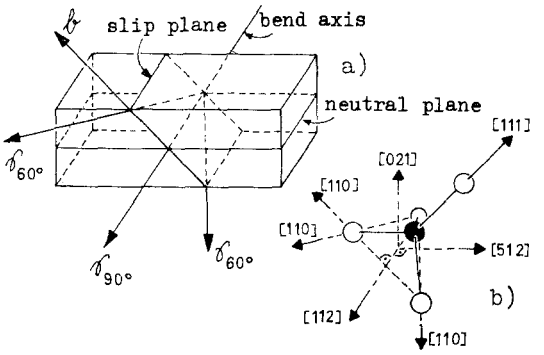

Figure 5 Crystallographic orientation of samples to produce single slip. Script b, Burger's vector, script γ, dislocation vectors.

During plastic bending, only one slip system is activated. This is shown in fig. 3, where the arrow-shaped etch pits revealed by modified CP4 are perpendicular to the lines of intersection between the (1 1 1) slip planes and the etched lateral (1 1 2) face of the sample.

The slip processes become more complicated when the crystallographic orientation of the samples is chosen according to fig. 6, since double slip occurs [7].

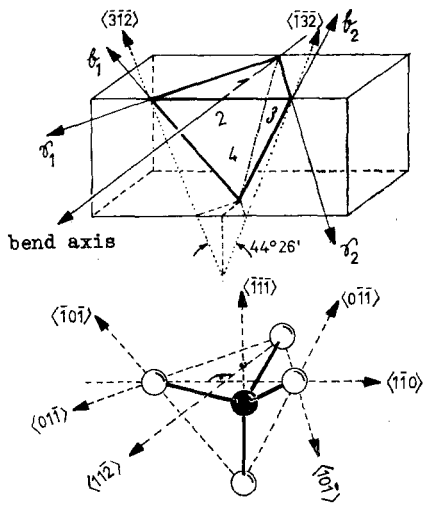

Figure 6 Crystallographic orientation of samples to produce double slip. 1 to 4, (111) planes, 2, 3, activated (111) slip planes, script b, Burger's vectors, script γ, dislocation vectors.

Therefore, the samples which were subsequently measured electrically were cut to produce single slip.

3.2. Electrical Measurement

3.2.1. Hall Coefficient Measurements

Vertically grown Ge-doped, InSb single crystals with an initial net impurity concentration $n_A - n_D = 4 \times 10^{13}$ cm^{-3} were supplied by the Mining and Chemical Products Ltd, Wembley.

In Ge-doped InSb, Cunningham *et al* found an acceptor level $E_A - E_V = 0.10$ eV, which they ascribed to the substitution of Sb by Ge atoms [24]. Bullis *et al* stated that the Ge atoms may also substitute In atoms [25]. They found a shallow donor level below the bottom of the conduction band, a shallow acceptor level above the top of the valence band, and the deep acceptor level measured by Cunningham *et al* [24]. It is possible, however, that the shallow levels of the Ge-doping and other impurity levels compensate each other, so that only the deep level $E_A - E_V = 0.10$ eV occurs. The starting material used showed this characteristic.

Fig. 7 shows the measured variation of the Hall coefficients with temperature. The parameter is the radius of curvature. It is shown, that the slope of the curves for an excess of In dislocations becomes steeper when the dislocation density is increased. The electrostatic charge per unit length of dislocation due to the dislocation-impurity interaction decreases when the dislocation density, i.e. the dislocation length per unit volume, is increased. Thus its influence on the measured energy level of the In dislocation states is reduced [26].

The curve for the maximum In dislocation density ($r_D = 5$ cm) shows an intersection with the curve for the undeformed material.* At low temperatures, the hole density of the dislocated crystal is lower than that of the undeformed material. This corresponds to a compensating donor action of the In dislocations. At higher temperatures, the hole density of the dislocated crystal is increased and surpasses that of the undeformed material according to an acceptor action of the In dislocations. This double action has already been observed for dislocations in p-type germanium [27].

For an excess of Sb dislocations, fig. 7 shows only an acceptor action. The hole density of the dislocated crystals is always superior to that of the undeformed material. The slope of the curves is nearly uniform at sufficiently low temperatures, i.e. the influence of the electrostatic charge per unit length of dislocation on the measured energy level of the Sb dislocation states is reduced compared with the case of In majority dislocations. This has already been observed for dislocations in Au-doped germanium, where the dislocation energy states lie below those of the chemical acceptors [28].

It is common to both types of dislocations, that the zero-axis crossing of the Hall coefficient is shifted to lower temperatures when the dislocation density is increased, due to the different scattering of holes and electrons at dislocations in the range of mixed conduction.

3.2.2. Conductivity Measurements and Hall Mobility

Fig. 8 shows the measured variation of the electrical conductivities with temperature. No significant difference can be seen between In and Sb majority dislocations. The conductivity decreases with increasing dislocation density.

The Hall mobilities $\mu_H = R_H\sigma$ derived from

*The starting material and the control samples were equal within ± 20%.

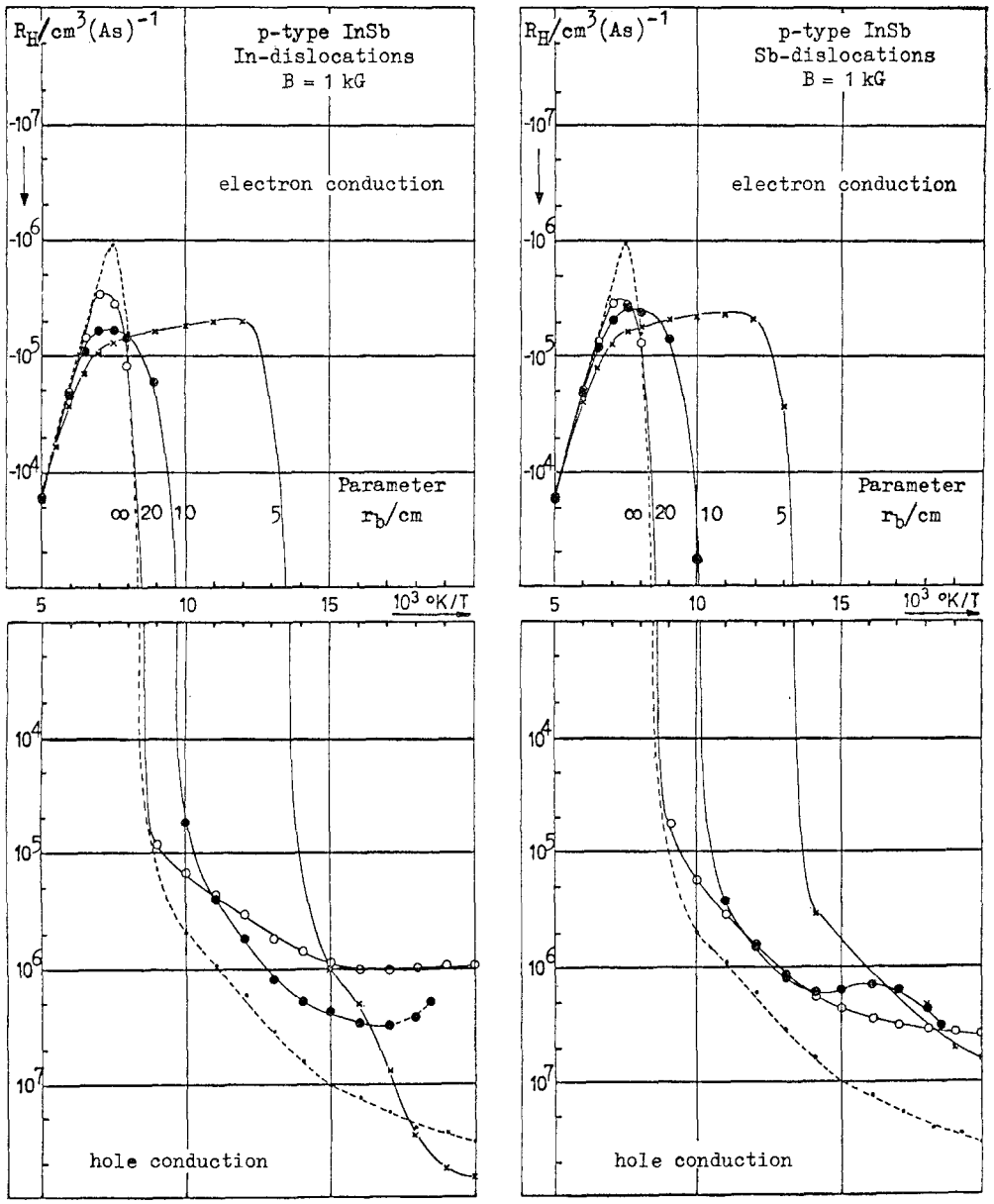

Figure 7 Measured variation of the Hall coefficients of unbent samples (dotted line, the starting material and the control samples were equal within ± 20%) and bent specimens of high dislocation density with temperature. Current density perpendicular, magnetic field vector parallel to dislocation lines.

the Hall effect and conductivity measurements are shown in fig. 9. The parameter is the radius of curvature. The curves can be divided into three ranges of temperature.

(*a*) *Extrinsic conduction.* At low temperatures, the Hall mobility is determined by the mobility of holes in the valence band. The curve of the undeformed material ($r_b = \infty$) shows hole scattering at ionised impurities and then follows the slope $\mu_{Lp}(T)$ evaluated by Putley [29] for the scattering of holes at thermal lattice vibrations. The absolute value of the Hall mobility decreases with increasing dislocation density by additional carrier scattering at charged dislocations. In the

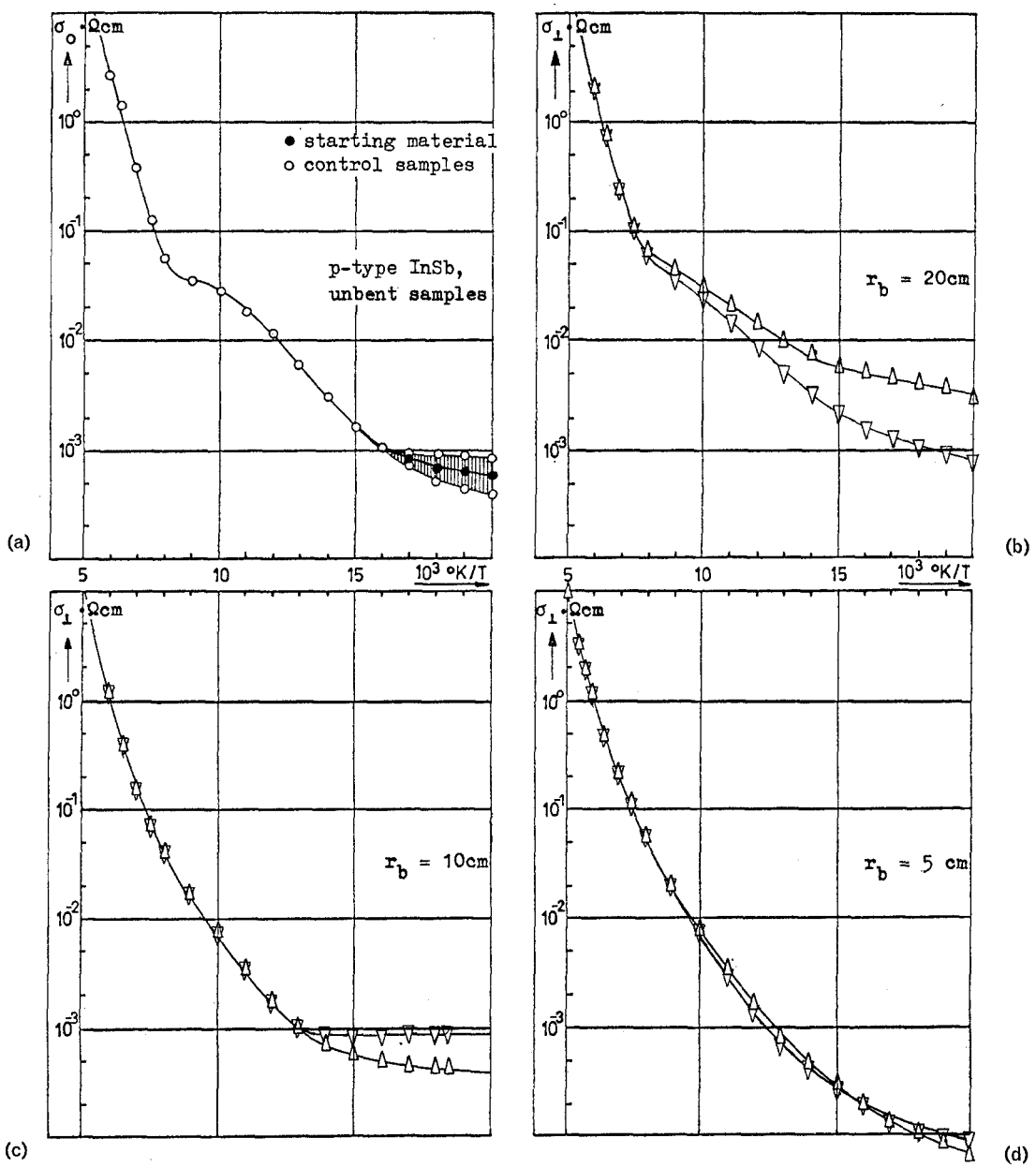

Figure 8 Measured variation of the electrical conductivities of unbent (a) and bent (b to d) specimens of high dislocation density with temperature. Current density perpendicular to dislocation lines. △ In excess dislocations, ▽ Sb excess dislocations.

range of donor action of In majority dislocations, however, relatively high Hall mobilities are measured.

(*b*) *Mixed conduction.* At medium temperatures, the measured Hall mobility is determined by slow holes in the valence band and rapid electrons activated from the valence into the conduction band by thermal energy. The sign of the Hall mobility depends on the ratio $p\mu_p^2$: $n\mu_n^2$ [30].

(*c*) *Intrinsic conduction.* At high temperatures, the electron density in the conduction band is increased by thermal activation, so that the Hall mobility is determined by the high electron

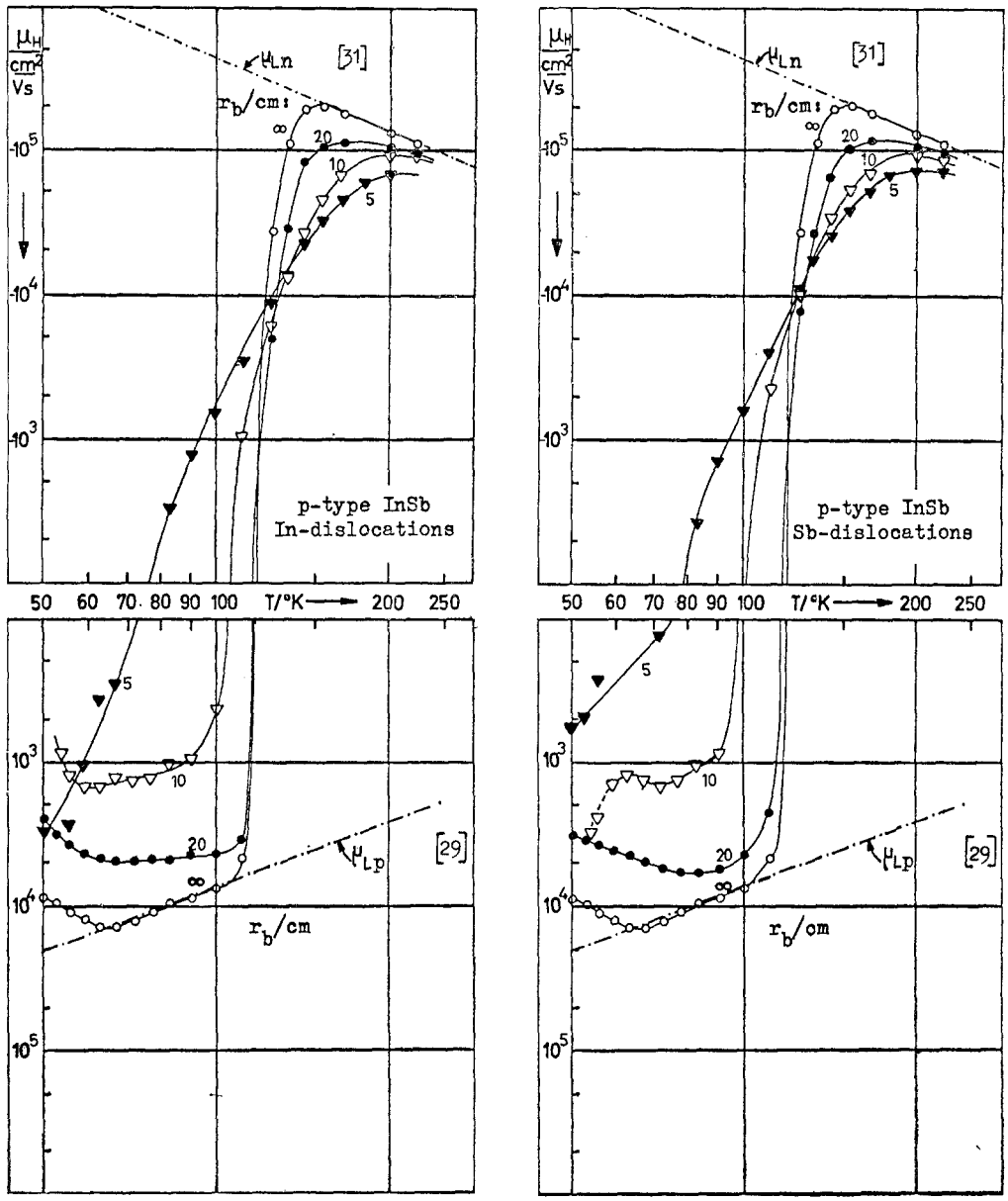

Figure 9 Temperature variation of Hall mobilities derived from measured Hall coefficients and electrical conductivities of unbent ($r_b = \infty$) and bent specimens with high dislocation density.

mobility in the conduction band. The curve of the undeformed material ($r_b = \infty$) follows the slope $\mu_{Ln}(T)$ evaluated by Putley [31] for the scattering of electrons at thermal lattice vibrations. The absolute value of the measured Hall mobility decreases again with increasing dislocation density, but the curves seem to approach the curve $\mu_{Ln}(T)$ at sufficiently high temperatures.

4. Conclusions and Summary

The electrostatic charge of the dislocations due to dislocation-impurity interaction has more influence on the measured energy level of In dislocations than on those of Sb. In addition, indium dislocations in Ge-doped InSb show not only an acceptor, but also a donor action, Sb dislocations showing only an acceptor action.

These results may be explained by assuming an energy level scheme in which the energy level of the In dislocation states lies above and that of the Sb dislocation states below the acceptor level $E_{AV} = 0.10$ eV of the Ge impurity atoms.

An In dislocation energy state above the impurity level causes a spontaneous compensation of the chemical acceptors by dangling bond electrons, without an external supply of energy. This corresponds to a donor action. When thermal energy is supplied, however, electrons are activated from the valence band into the In dislocation states, corresponding to an acceptor action. The activation energy is higher than that of the Ge acceptors. Therefore the slope of the Hall coefficient characteristic $R_H(1/T)$ is steeper than that of the undeformed, Ge-doped material, when the influence of the electrostatic charge is low enough.

An Sb dislocation energy state below the impurity level cannot produce the effect of spontaneous compensation of chemical acceptors. When external energy is supplied, electrons are activated from the valence band into the Sb dislocation states due to their acceptor action. The slope of the Hall coefficient characteristic $R_H(1/T)$ is shallower than that of the undeformed material in the extrinsic conduction range, since the dislocation activation energy is lower than that of the Ge acceptors.

These effects can only be observed when the density of the dislocation states is higher than the impurity concentration.

Acknowledgement

The authors express their grateful thanks to Professor Dr W. Güth for many useful discussions. We are indebted to Professor Dr J. Dosse for provision of laboratory facilities.

References

1. D. B. HOLT, *J. Phys. and Chem. Solids* **23** (1962) 1353.
2. P. HAASEN, *Acta Metallurgica* **5** (1957) 598.
3. J. J. DUGA, *Bull. Amer. Phys. Soc.* Ser. II **3** (1958) 378.
4. H. C. GATOS and M. C. FINN, *J. Metals* **13** (1961) 77.
5. J. J. DUGA, *ibid* **13** (1961) 77.
6. H. C. GATOS, M. C. FINN, and M. C. LAVINE, *J. Appl. Phys.* **32** (1961) 1174.
7. J. J. DUGA, *ibid* **33** (1962) 169.
8. R. K. MUELLER and R. L. JACOBSON, *ibid* **33** (1962) 2341.
9. R. M. BROUDY, *Adv. Phys.* **12** (1963) 135.
10. R. K. MUELLER and K. N. MAFFITT, *J. Appl. Phys.* **35** (1964) 734.
11. R. L. BELL, R. LATKOWSKI, and A. F. W. WILLOUGHBY, *J. Materials Sci.* **1** (1966) 66.
12. S. AMÉLINCKX, "Solid-State Physics", Supplement 6 (Academic Press, New York/London, 1964).
13. J. F. NYE, *Acta Metallurgica* **1** (1953) 153.
14. J. J. DUGA, R. K. WILLARDSON, and A. C. BEER, *J. Appl. Phys.* **30** (1959) 1798.
15. H. C. GATOS and M. C. LAVINE, *J. Electrochem. Soc.* **107** (1960) 427.
16. H. L. HENNEKE, *J. Appl. Phys.* **36** (1965) 2967.
17. H. C. GATOS and M. C. LAVINE, *J. Phys. and Chem. Solids* **14** (1960) 169.
18. E. PEISSKER, P. HAASEN, and H. ALEXANDER, *Phil. Mag.* (8) **7** (1962) 1279.
19. M. WILHELM (private communication).
20. B. I. BOLTAKS and V. I. SOKOLOV, *Soviet Phys.-Sol. St.* **5** (1963) 785.
21. I. A. GUSEV and A. N. MURIN, *ibid* **6** (1964) 932.
22. R. B. DZHANELIDZE and N. I. KURDIANI, *ibid* **5** (1963) 501.
23. M. C. LAVINE, H. C. GATOS, and M. C. FINN, *J. Electrochem. Soc.* **108** (1961) 974.
24. R. W. CUNNINGHAM, E. E. HARP, and W. M. BULLIS, Proc. Int. Conf. Semiconductor Physics, Exeter (The Institute of Physics and The Physical Society, London, 1962) p. 732.
25. W. M. BULLIS and V. HARRAP, Proc. Int. Conf. Physics of Semiconductors, Paris (Dunod, Paris, 1964) p. 847.
26. W. T. READ JR, *Phil. Mag.* (7) **45** (1954) 775.
27. W. SCHRÖTER, *Phys. Stat. Sol.* **21** (1967) 211.
28. A. G. TWEET, *Phys. Rev.* **99** (1955) 1245.
29. E. H. PUTLEY, *Proc. Phys. Soc.* **73** (1959) 128.
30. O. MADELUNG and H. WELKER, *Z. angew. Phys.* **5** (1953) 12.
31. E. H. PUTLEY, *Proc. Phys. Soc.* **73** (1959) 280.